Research Paper
Computational Methods for Differential Equations
http://cmde.tabrizu.ac.ir
Vol. *, No. *, *, pp. 1-13
DOI:10.22034/cmde.2026.70421.3501

Numerical approximation of cubic nonlinear Schrödinger equation using local Fourier based differential quadrature method (L-DQM)

Meirikim Panmei and Roshan Thoudam*

Department of Mathematics, Manipur University, Canchipur-795003, Manipur, India.

Abstract

This paper introduces a numerical method to address the one-dimensional nonlinear Schrödinger equation, utilizing a localized differential quadrature scheme derived from Fourier series expansion to estimate the solutions. A Runge-Kutta fourth-order (RK4) method is used for time integration. To evaluate the accuracy and efficiency of the current approach, calculations have been performed for the error norm and the two lowest invariants, C_1 and C_2. The numerical results obtained were compared with earlier studies, and the findings clearly demonstrate that the present method is stable, accurate and highly effective numerical scheme.

Keywords. Cubic nonlinear Schrödinger equation, Fourier series expansion, Differential quadrature method, RK4, Soliton.
2010 Mathematics Subject Classification. 65M99, 42A38, 35Q55.

Uncorrected P

1. Introduction

In recent decades, solving differential equations numerically has become a focal point of interest in scientific computation [7, 24, 25]. The nonlinear Schrödinger (NLS) equation effectively describes various natural phenomena, including the optical pulse dynamics, water waves, plasma waves and the focusing behavior of laser beams. Consequently, researchers have focused on both analytical and numerical solutions to the NLS equation [6, 21]. Robinson [12] applied the orthogonal spline collocation method to nonlinear Schrödinger equations, demonstrating its accuracy and conservation properties. Twizell et al.[22] developed a finite difference method for solving the cubic Schrödinger equation, analyzing stability and convergence through Padé approximants. Muslu and Erbay [10] employed split-step Fourier methods of various orders (first, second, and fourth) for the numerical solution of the generalized nonlinear Schrödinger (GNLS) equation. A Taylor collocation method with a quintic B-spline basis for the nonlinear Schrödinger equation was presented in [1]. Bashan [2] also proposed a mixed method based on the finite difference scheme and quartic B-spline differential quadrature for solving the Schrödinger equation. Due to its significance, extensive efforts have been directed toward developing diverse techniques to analyze and solve the NLS equation, including finite difference method, quadratic finite element method (FEM), and quintic B-spline based FEM etc. [5, 13, 22].

One notable form of the NLSE is the cubic nonlinear Schrödinger equation (CNLS), expressed as:

$$i\psi_t + \psi_{xx} + p|\psi|^2\psi = 0, \qquad x \in [a, b],\ t \geq 0, \tag{1.1}$$

where $i = \sqrt{-1}$, p is a real parameter. Meanwhile the subscripts x and t describe partial derivatives w.r.t spatial and temporial variables, respectively which has applications in nonlinear optics [20], plasma physics [14] and fluid dynamics [9].

The organization of this paper is as follows: Sections 2 and 3 introduce the basic concepts of DQM along with the local Fourier-based differential quadrature technique. In Section 4, the implementation of CNLS equation is discussed. Section 5 focuses on the stability investigation of the scheme whereas Section 6 presents numerical simulations for

Received: 27 November 2025; Accepted: 29 October 2026.
∗ Corresponding author. Email: roshan.dmc@gmail.com.

certain test cases . Further numerical studies and corresponding results are discussed in Sections 6.1 through 6.4. Finally, Section 7 provides concluding observations.

2. Differential Quadrature Method (DQM)

Bellman et al.[3] introduced the DQM in 1972 as a powerful tool for numerically solving complex differential equations. The core idea behind this method is to estimate a derivative at a given location through a weighted sum of the function values evaluated at specific collocation nodes. A fundamental aspect of this methodology is the determination of weighting coefficients, which are essential for achieving accurate results. Numerous scholars have employed various test functions to develop distinct DQM, including Legendre polynomials, spline functions, Chebyshev polynomials, etc. [4, 11, 18, 23]. Shu proposed an improved method for calculating weighting coefficients [15]. In their work, Shu and Rechards [17] utilized Lagrange interpolating polynomials, which allow for flexible selection of grid points. This approach resulted in the development of the polynomial-based differential quadrature (PDQ) method. Additionally, a recursive scheme was devised for evaluating the coefficients corresponding to higher-order derivatives. If Fourier series expansion is used in place of polynomials, the technique is categorized as the Fourier-based differential quadrature (FDQ) method. Based on DQ theory [16], the n^{th} order derivative of $\mathcal{U}(x,t)$ w.r.t. x at a point x_i over the finite interval $a = x_1 < x_2 < \cdots < x_N = b$ is :

$$\mathcal{U}^{(n)}(x_i,t) = \sum_{j=1}^{N} g_{i,j}^{(n)} \mathcal{U}(x_j,t), \qquad n = 1,\ldots,N-1 \text{ and } i,j = 1,\ldots,N, \tag{2.1}$$

where $g_{i,j}^{(n)}$ is the weighting coefficients and N is the number of subintervals in which the solution domain $[a,b]$ is divided.

3. Local Fourier-based DQM (L-DQM)

We take a partition $a = x_1 < x_2 < \cdots < x_i < \cdots < x_N = b$ of the domain [a,b] and the set of base functions are [16]

$$1, \cos\left(\frac{\pi x}{L}\right), \sin\left(\frac{\pi x}{L}\right), \ldots, \cos\left(\frac{(N-1)\pi x}{2L}\right), \sin\left(\frac{(N-1)\pi x}{2L}\right), \tag{3.1}$$

and

$$h_j(x) = \frac{G(x)}{\sin\left(\frac{\pi(x-x_j)}{2L}\right) G^{(1)}(x_j)}, \quad x \in [a,b], \tag{3.2}$$

where

$$G(x) = \prod_{m=1}^{N} \sin\left(\frac{\pi(x-x_m)}{2L}\right),$$

$$G^{(1)}(x_j) = \prod_{m=1, m\neq j}^{N} \sin\left(\frac{\pi(x_j-x_m)}{2L}\right), \; x \in [a,b],$$

$$L = (b-a).$$

The weighting coefficient for both 1^{st} and 2^{nd} order derivatives, by Shu [16]

$$\begin{cases} g_{i,j}^{(1)} = \frac{\pi}{2L} \frac{G^{(1)}(x_i)}{\sin\left(\frac{\pi(x_i-x_j)}{2L}\right) G^{(1)}(x_j)}, & i \neq j, \\ g_{i,j}^{(2)} = g_{i,j}^{(1)} \left(2g_{i,i}^{(1)} - \frac{\pi}{L} \cot\left(\frac{\pi(x_i-x_j)}{2L}\right)\right), & i \neq j, \\ g_{i,i}^{(n)} = -\sum_{j=1, j\neq i}^{N} g_{i,j}^{(n)}, & n = 1,2, \end{cases} \tag{3.3}$$

where $i,j = 1,2,\ldots,N$. To approximate the derivative of the unknown function, we used equally spaced grid points. Following the approach used by Shu [16], we focus on a specific spatial point x_i, where $i = 1,2,\ldots,N$.

Uncorrected Proof

At each of this points, we construct a stencil $\mathbf{S}_i = \{x_{i-M_1}, x_{i-M_1+1}, \ldots, x_{i-1}, x_i, \ x_{i+1}, \ldots x_{i+M_2}\}$ consisting of $M+1$ neighbouring nodes, where $M = M_1 + M_2$. For the left boundary point x_1, we set $M_1 = 0$ and $M_2 = M$. In contrast, for the right boundary point x_N, we set $M_1 = M$ and $M_2 = 0$. Using the $M+1$ surrounding nodes $\{x_{i-M_1}, x_{i-M_1+1}, \ldots, x_{i-1}, x_i, x_{i+1}, \ldots, x_{i+M_2}\}$, we calculate the n$^{\text{th}}$ order spatial derivative of $\mathcal{U}(x,t)$ at x_i using the expression below:

$$\mathcal{U}_x^{(n)}(x_i,t) = \sum_{j=-M_1}^{M_2} g_{i,i+j}^{(n)} \mathcal{U}(x_{i+j},t), \tag{3.4}$$

the weighting coefficients for the 1^{st} and 2^{nd} order derivatives in the L-DQM scheme are expressed as follows

$$g_{i,i+j}^{(1)} = \frac{\pi}{2L} \frac{G^{(1)}(x_i)}{\sin\left(\frac{\pi(x_i - x_{i+j})}{2L}\right) G^{(1)}(x_{i+j})}, \quad \text{for } j \neq 0, \quad j = -M_1, \ldots, M_2. \tag{3.5}$$

where,

$$G^{(1)}(x_i) = \prod_{\substack{m=M_1 \\ m\neq 0}}^{M_2} \sin\left(\frac{\pi(x_i - x_{i+m})}{2L}\right),$$

and

$$G^{(1)}(x_{i+j}) = \prod_{\substack{m=-M_1 \\ m\neq j}}^{M_2} \sin\left(\frac{\pi(x_{i+j} - x_{i+m})}{2L}\right),$$

$$g_{i,i+j}^{(2)} = g_{i,i+j}^{(1)} \left(2g_{i,i}^{(1)} - \frac{\pi}{L} \cot\left(\frac{\pi(x_i - x_{i+j})}{2L}\right)\right), \ j \neq 0, \ j = -M_1, \ldots, M_2. \tag{3.6}$$

For the diagonal coefficients $g_{i,i}^{(n)}$, we have

$$g_{i,i}^{(n)} = - \sum_{\substack{m=-M_1, \\ m\neq 0}}^{M_2} g_{i,i+m}^{(n)}, \quad n = 1, 2. \tag{3.7}$$

After obtaining the weighting coefficients, the differentiation matrices $\mathcal{W}^{(1)} = \left(g_{i,j}^{(1)}\right)_{N\times N}$ and $\mathcal{W}^{(2)} = \left(g_{i,j}^{(2)}\right)_{N\times N}$ are formulated to approximate the 1^{st} and 2^{nd} spatial derivatives of $\mathcal{U}(x,t)$ over the interval [a, b].

4. Implementation

In this section, the CNLS equation is examined under the following initial and boundary conditions defined on the domain $a \leq x \leq b$:

$$\psi(x,0) = f(x), \ a \leq x \leq b, \tag{4.1}$$

$$\psi(a,t) = \psi(b,t) = 0, \ 0 < t \leq T. \tag{4.2}$$

By defining $\psi(x,t) = r(x,t) + is(x,t)$, we can effectively transform the CNLS Eq. (1.1) along with the IC Eq. (4.1) and BC Eq. (4.2) into a comprehensive coupled initial-boundary value problem (IBVP)

$$\begin{cases} r_t = -s_{xx} - p(r^2+s^2)s, \\ s_t = r_{xx} + p(r^2+s^2)r. \end{cases} \tag{4.3}$$

The ICs are:

$$r(x,0) = r_0(x), \ s(x,0) = s_0(x), \ a \leq x \leq b, \tag{4.4}$$

Uncorrected Proof

and the BCs are:

$$r(a,t) = r(b,t) = 0,\ \ s(a,t) = s(b,t) = 0,\ \ 0 < t \leq T. \tag{4.5}$$

To solve system Eq. (4.3) subject to the ICs Eq. (4.4) and BCs Eq. (4.5) at the collocation points $x_1, x_2, \ldots, x_N$, a uniform step size $h = x_{i+1} - x_i$, is employed for $i = 1, 2, \ldots, N-1$, we define

$$\mathbb{U}(t) = [r_1(t), r_2(t), \ldots, r_N(t)]^T,$$

$$\mathbb{V}(t) = [s_1(t), s_2(t), \ldots, s_N(t)]^T,$$

where $r_i(t) = r(x_i, t),\ s_i(t) = s(x_i, t)$ for all $i = 1, 2, \ldots, N$.
By employing the differentiation matrices $\mathcal{W}^{(1)}$ and $\mathcal{W}^{(2)}$ (Section 3), the system of PDEs Eq. (4.3) are transformed into a system of ODEs, which can be represented in matrix form.

$$\begin{cases} \mathbb{U}'(t) = -\mathcal{W}^{(2)}.\mathbb{V}(t) - \left[p\left(\mathbb{U}^2(t) + \mathbb{V}^2(t)\right)\right] * \mathbb{V}(t), \\ \mathbb{V}'(t) = \mathcal{W}^{(2)}.\mathbb{U}(t) + \left[p\left(\mathbb{U}^2(t) + \mathbb{V}^2(t)\right)\right] * \mathbb{U}(t), \end{cases} \tag{4.6}$$

where $\mathbb{U}(t) * \mathbb{V}(t)$, $\mathbb{U}^2(t) = \mathbb{U}(t) * \mathbb{U}(t)$ etc. denotes component by component multiplication of two matrices, while a dot $(\cdot)$ represents standard matrix multiplication. Using the corresponding ICs from Eq. (4.4) and BCs from Eq. (4.5), we solve the system of ODEs described in Eq. (4.6) using the standard Runge-Kutta fourth-order (RK4) method.

5. Stability Analysis

In order to examine the stability of the method, Eq. (4.3) is expressed in matrix form as [19]:

$$\frac{dX}{dt} = AX + \Phi(X), \tag{5.1}$$

where

$$A = \begin{bmatrix} 0 & -D \\ D & 0 \end{bmatrix}_{2N \times 2N}, X = \begin{bmatrix} r_i & s_i \end{bmatrix}^T_{2N \times 1},$$

$$\Phi(X) = \begin{bmatrix} y_i(X) & z_i(X) \end{bmatrix}^T_{2N \times 1},$$

$$y_i(X) = -p(r_i^2 + s_i^2)s_i,\ \ z_i(X) = p(r_i^2 + s_i^2)r_i,\ \ i = 1, 2, \ldots, N,$$

$$D = \begin{bmatrix} g_{11}^{(2)} & g_{12}^{(2)} & \cdots & g_{1N}^{(2)} \\ g_{21}^{(2)} & g_{22}^{(2)} & \cdots & g_{2N}^{(2)} \\ g_{31}^{(2)} & g_{32}^{(2)} & \cdots & g_{3N}^{(2)} \\ \vdots & \vdots & \ddots & \vdots \\ g_{N1}^{(2)} & g_{N2}^{(2)} & \cdots & g_{NN}^{(2)} \end{bmatrix}.$$

Here, 0 denotes a null matrix, and X represents the solution vector corresponding to r and s. It is evident that the system admits $(0, 0)$ as a simple critical point. To establish stability, it is required to verify the condition

$$\lim_{X \to 0} \frac{\Phi(X)}{\|X\|} = 0.$$

The proof is carried out only for $y_i(X)$, since once this case is established, the result for $z_i(X)$ follows directly.

$$\begin{aligned} \left\| \frac{y_i(X)}{\sqrt{r_1^2 + r_2^2 + \cdots + r_N^2 + s_1^2 + s_2^2 + \cdots + s_N^2}} - 0 \right\| &= \left\| \frac{-p(r_i^2 + s_i^2)s_i}{\sqrt{r_1^2 + r_2^2 + \cdots + r_N^2 + s_1^2 + s_2^2 + \cdots + s_N^2}} \right\| \\ &\leq \|p\| \|r_1^2 + r_2^2 + \cdots + r_N^2 + s_1^2 + s_2^2 + \cdots + s_N^2\| \\ &\leq \epsilon, \end{aligned}$$

Uncorrected Proof

for all $\epsilon > 0$, we have $\delta^2 = \frac{\epsilon}{p}$, so that

$$\left\| \frac{y_i(X)}{\sqrt{r_1^2 + r_2^2 + \cdots + r_N^2 + s_1^2 + s_2^2 + \cdots + s_N^2}} - 0 \right\| \leq \epsilon,$$

whenever

$$\sqrt{r_1^2 + r_2^2 + \cdots + r_N^2 + s_1^2 + s_2^2 + \cdots + s_N^2} \leq \delta.$$

Hence,

$$\lim_{X \to 0} \frac{\Phi(X)}{\|X\|} = 0.$$

At that point, the stability of nonlinear system Eq. (4.3) is identical with the stability of related linear system,

$$\frac{dX}{dt} = AX.$$

The stability of this linear system can be assessed by analyzing the eigenvalues of the coefficient matrix A. The system is stable or asymptotically stable if all eigenvalues of A have non-positive or strictly negative real parts [19]. For the problems under consideration, the proposed method is shown to be stable, as all eigenvalues of the coefficient matrix A possess non-positive real parts, as illustrated in Figure 12.

6. Numerical experiment

The accuracy and effectiveness are demonstrated using four test problems. We measure its accuracy with the L_∞ error norm, which is defined as follows:

$$L_\infty = \max_{1 \leq i \leq N} \left| \, |\psi(i)|_{exact} - |\psi(i)|_{approximate} \right|. \tag{6.1}$$

The two lowest invariants are given below:

$$C_1 = \int_a^b |\psi|^2 dx,$$
$$C_2 = \int_a^b |\psi_x|^2 - \frac{1}{2} p |\psi|^4 dx.$$

6.1. **Single solitary wave solution:** The initial numerical test explores the propagation behavior of a single soliton, for which an exact analytical expression is of the form [2]

$$\psi(x,t) = \gamma \sqrt{\frac{2}{p}} \exp i \left\{ \frac{2Sx - (S^2 - \gamma^2)t}{4} \right\} \operatorname{sech} \gamma(x - St), \tag{6.2}$$

where S represents the speed of a single soliton, with its amplitude depending on γ. The parameters for this test are set as: $p = 2$, $S = 4$, and $\gamma = 1$ and 2, over the domain $[-20, 20]$, to facilitate direct comparison with previous works [5, 6]. For performance assessment, the values of L_∞, C_1 and C_2 are compared against those obtained by the FDM-DQM [2] and quadratic B-spline-based finite element method [5] using $\Delta t = 0.005$ and $N = 291$, as shown in Table 1. The motion of single soliton at different time is shown in Figures 1 and 2. It is evident from Table 1 that, by using the same parameters and nodal points [2], the new results outperform those obtained using the FDM-DQM, quadratic B-spline-based finite element method and others. Moreover, as the time step is reduced, the error in the L_∞ norm produced by the L-DQM method decreases significantly, reaching as low as 2.9×10^{-7} at $t = 0.5$ with stencil sizes $M = 10$. These are the best results in this presented method. Likewise, when the soliton amplitude is increased to $\gamma = 2$, the outcomes provided in Table 2 at time $t = 1$ surpass all previously documented results for the NLSE.

Uncorrected Proof

TABLE 1. Evaluation of error norms and invariants at Δt =0.005.

t	Present (L-DQM) N=291			FDM-DQM [2] N=291			Quad. FEM [5] N=800		
	C_1	C_2	L_∞	C_1	C_2	L_∞	C_1	C_2	L_∞
0.0	1.99947	7.33054	0.00000	2.00000	7.33370	0.00000	2.0	7.3537736	0.0000
0.5	1.99947	7.33054	2.9×10^{-7}	2.00000	7.33371	8.0×10^{-5}	2.0	7.3537756	2.0×10^{-4}
1.0	1.99947	7.33054	5.7×10^{-7}	2.00001	7.33373	1.5×10^{-4}	2.0	7.3537778	3.0×10^{-4}
1.5	1.99947	7.33054	6.2×10^{-6}	2.00001	7.33374	2.1×10^{-4}	2.0	7.3537793	4.0×10^{-4}
2.0	1.99947	7.33054	3.2×10^{-5}	2.00001	7.33375	2.6×10^{-4}	2.0	7.3537802	5.0×10^{-4}
2.5	1.99947	7.33054	1.8×10^{-4}	2.00001	7.33377	2.9×10^{-4}	2.0	7.3537803	6.0×10^{-4}

TABLE 2. Comparison of L_∞ error of single soliton at amplitude, γ =2 and t=1.

Method	N	Δt	L_∞
L-DQM	386	0.005	0.00020
L-DQM	391	0.0048	0.00019
FDM-DQM [2]	386	0.005	0.00031
FDM-DQM [2]	391	0.0048	0.00028
Quad. Gal.[5]	386	0.005	0.0004
Quad. Gal.[5]	391	0.0048	0.004

Uncorrected Proof

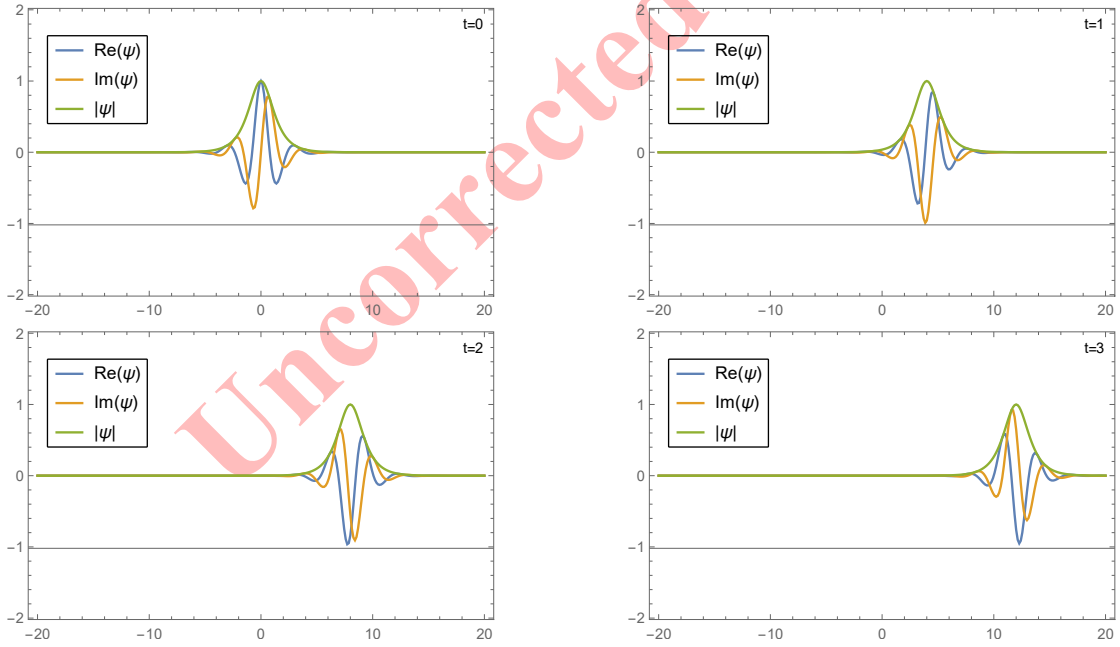


FIGURE 1. Single soliton at $\Delta t = 0.005, N = 291$.

6.2. **Interaction of two solitons:** The IC for the collision of double solitons is as follows [6]:

$$\psi(x,0) = \psi_1(x,0) + \psi_2(x,0), \tag{6.3}$$

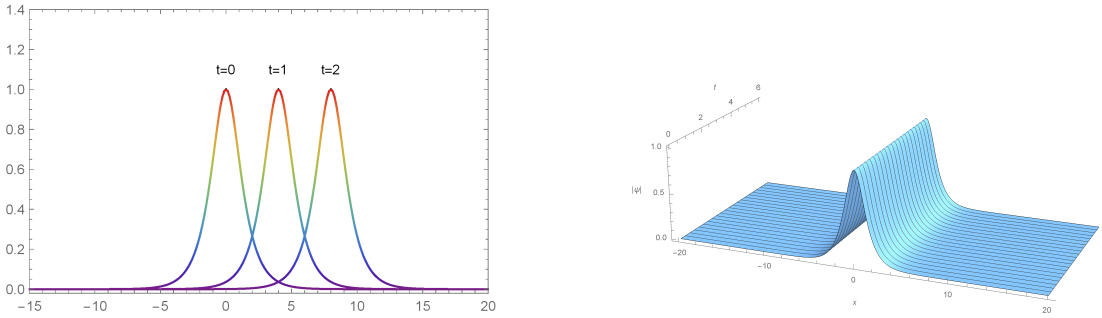


FIGURE 2. Solitary wave at different time levels.

TABLE 3. Invariants of double solitons at $\gamma_1 = \gamma_2 = 1$.

t	Present (L-DQM)		FDM-DQM [2]		Quad.Gal.[5]	
	C_1	C_2	C_1	C_2	C_1	C_2
0.0	3.999590	14.66450	3.999998	14.66677	3.99999	14.83143
0.5	3.999590	14.66520	3.999996	14.66668	3.99999	14.83150
1.0	3.999590	14.66620	3.999999	14.66668	3.99999	14.83157
1.5	3.999580	14.66700	4.000000	14.66667	3.99999	14.83161
2.0	3.999580	14.66770	3.999998	14.66668	3.99999	14.83261
2.5	3.999240	14.67860	3.999994	14.66672	3.99999	14.95380
3.0	3.999580	14.66800	3.999998	14.66667	3.99999	-
3.5	3.999580	14.66730	3.999999	14.66668	3.99999	14.83161
4.0	3.999590	14.66670	3.999996	14.66668	3.99999	14.83158
4.5	3.999590	14.66610	3.999997	14.66669	3.99999	14.83156
5.0	3.999600	14.66570	3.999997	14.66667	3.99999	14.83153
5.5	3.999600	14.66550	3.999999	14.66676	4.00000	14.83153

Uncorrected Proof

where,

$$\psi_1(x,0) = \gamma_1\sqrt{\frac{2}{p}}\exp i\left\{\frac{\sigma_1}{2}(x-x_1)\right\}.\operatorname{sech}\gamma_1(x-x_1),$$

and

$$\psi_2(x,0) = \gamma_2\sqrt{\frac{2}{p}}\exp i\left\{\frac{\sigma_2}{2}(x-x_2)\right\}.\operatorname{sech}\gamma_2(x-x_2).$$

We have set the values of $p = 2$, $\gamma_1 = \gamma_2 = 1$, $\sigma_1 = -4$, $\sigma_2 = 4$, $x_1 = 10$ and $x_2 = -10$ over the interval $-20 \le x \le 20$. This simulation illustrates the collision of two solitons located at positions $x_1 = 10$ and $x_2 = -10$, moving toward each other with the same amplitude ($\gamma_1 = \gamma_2 = 1$) and the same speed ($\sigma_1 = \sigma_2 = 4$). Due to the unique characteristics of solitons, they preserve their properties such as shape, speed and amplitude after the collision, as evidenced by the simulations of the double solitons shown in Figure 4. The simulations are conducted up to a time of $t = 5.5$. Around $t = 2$, the solitons begin to interact, and the peak amplitude rises to approximately $\gamma = 2$ by $t = 2.5$. After the interaction concludes at $t = 5.5$, both solitons are seen to preserve their original form and trajectory. Table 3 displays the two lowest invariants of the method, offering a comparison with previous studies using a stencil size $M = 2$. At time $t = 2.5$, the changes in the invariants, C_1 and C_2 are particularly important for the efficiency of the implemented methods. The outcomes shown in Table 3 demonstrate that the present L-DQM implementation delivers more accurate invariant preservation during collision than the previously published results.

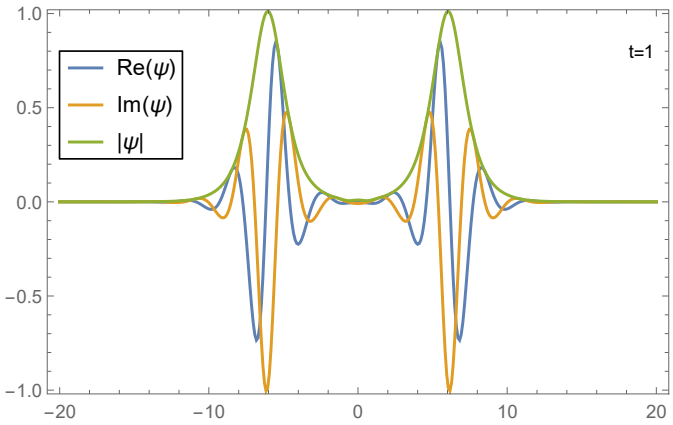
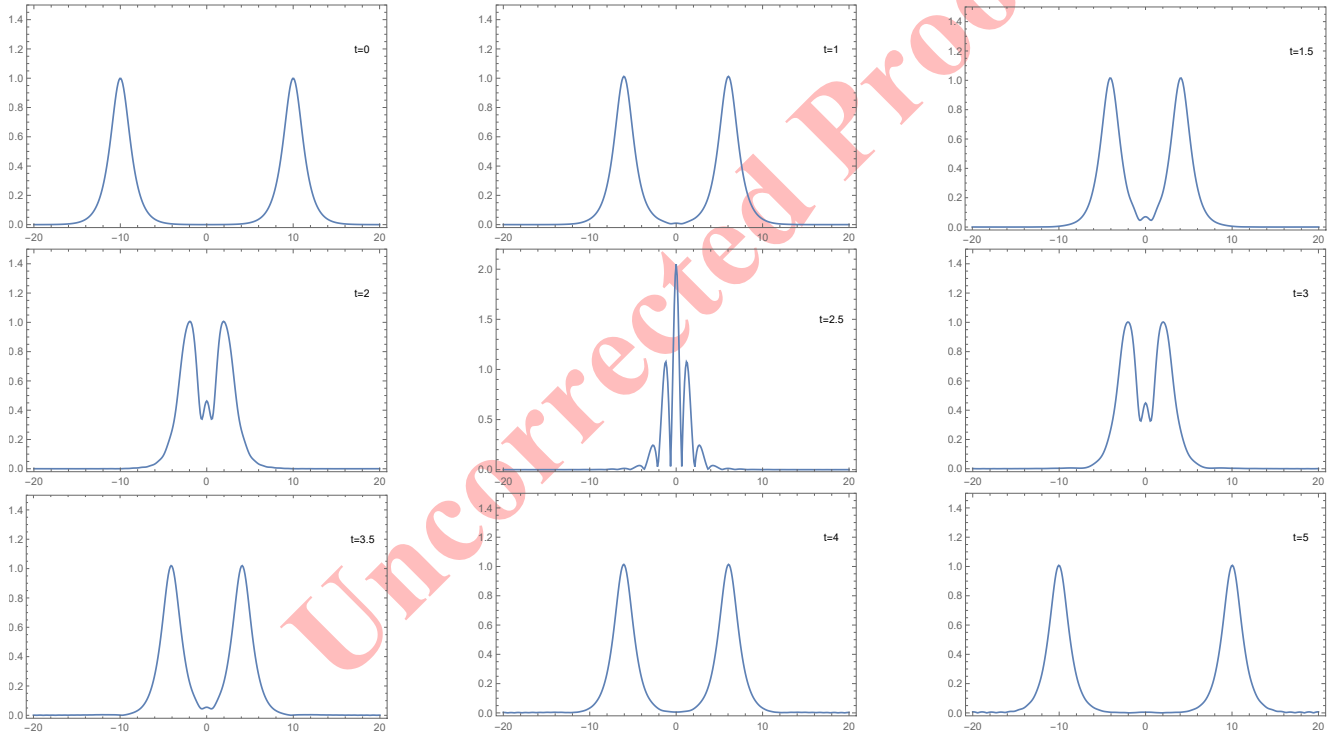


FIGURE 3. Double solitons at $\gamma_1 = \gamma_2 = 1$.



Uncorrected Proof

FIGURE 4. Interaction of two solitons(N=341, $\Delta t = 0.005$).

6.3. **Standing soliton:**

$$\text{If } \int_{-\infty}^{\infty} \psi(x,0)dx \geq \pi, \tag{6.4}$$

then the IC $\psi(x,0)$ will effectively produce a soliton, in contrast, if this condition is not satisfied, the soliton will decay. Defour et al.[6] conducted a comprehensive study on soliton formation utilizing a square-well IC. Similarly, Gardner

TABLE 4. Invariants of standing solitons at $E = 1$ and $E = 1.78$.

t	E=1		E=1.78	
	C_1	C_2	C_1	C_2
0.0	1.25326	0.36699	3.97091	-4.92517
0.5	1.25329	0.36695	3.97076	-4.92379
1.0	1.25330	0.36695	3.97080	-4.92420
1.5	1.25330	0.36696	3.97079	-4.92411
2.0	1.25330	0.36696	3.97078	-4.92405
2.5	1.25330	0.36696	3.97079	-4.92411
3.0	1.25330	0.36696	3.97079	-4.92412
3.5	1.25330	0.36696	3.97078	-4.92407
4.0	1.25330	0.36696	3.97079	-4.92407
4.5	1.25330	0.36697	3.97080	-4.92402
5.0	1.25330	0.36698	3.97082	-4.92387
5.5	1.25330	0.36697	3.97088	-4.92372

et al.[8] examined the same phenomenon using a Maxwellian IC defined by

$$\psi(x, 0) = E \exp(-x^2). \tag{6.5}$$

For the Maxwellian IC, the parameters used were $\Delta t = 0.4$ and $p = 2$, within the interval $[-45, 45]$, to demonstrate the formation of a soliton. A numerical experiment was conducted up to the time $t = 5.5$ with values $E = 1$ and $E = 1.78$. The results shown in figures indicate that the initial pulse fades away when $E = 1$, while at $E = 1.78$, a soliton with a magnitude of approximately two develops. A standing soliton is depicted in Figure 7 and Figure 8 for $M = 4$. It is important to note that when $E = 1.78$ exceeds the threshold value $\sqrt{\pi} \approx 1.7725$, it leads to soliton formation. Numerical results have been computed for $E = 1$ with $\Delta t = 0.01$ and $N = 611$, as well as for $E = 1.78$ with $\Delta t = 0.005$ and $N = 721$. These results are illustrated in Table 4. It can be observed that the method used produces two invariants, C_1 and C_2, which remain nearly constant and show good accuracy.

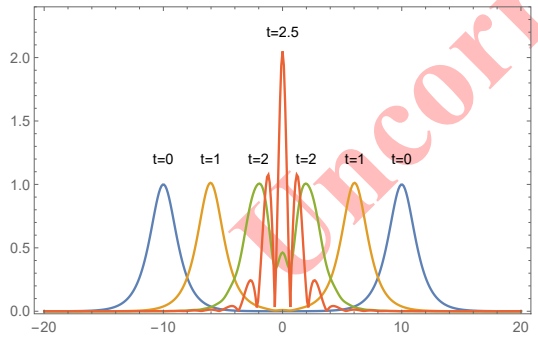


FIGURE 5. Interaction of two solitons (N=341, $\Delta t = 0.005$).

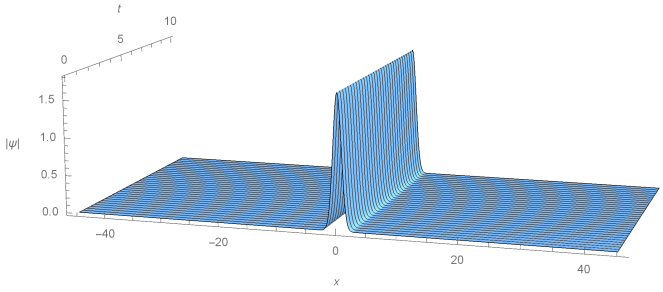


FIGURE 6. 3D of standing soliton at $t = 1$.

6.4. **Mobile soliton:** The mobile soliton is utilized with the following IC [2]:

$$\psi(x, 0) = E \exp(-x^2 + 2ix), \tag{6.6}$$

with the parameter $p = 2$ in the interval $[-45, 45]$. The characteristics of the solutions for $E = 1$ and $E = 1.78$ are illustrated in the Figure 9 and Figure 10 respectively with $M = 2$. When $E = 1$, the amplitude of $|\psi|$ gradually diminishes over time, as reflected in the plots. Conversely, when $E = 1.78$, the soliton retains its amplitude, shape and

Uncorrected Proof

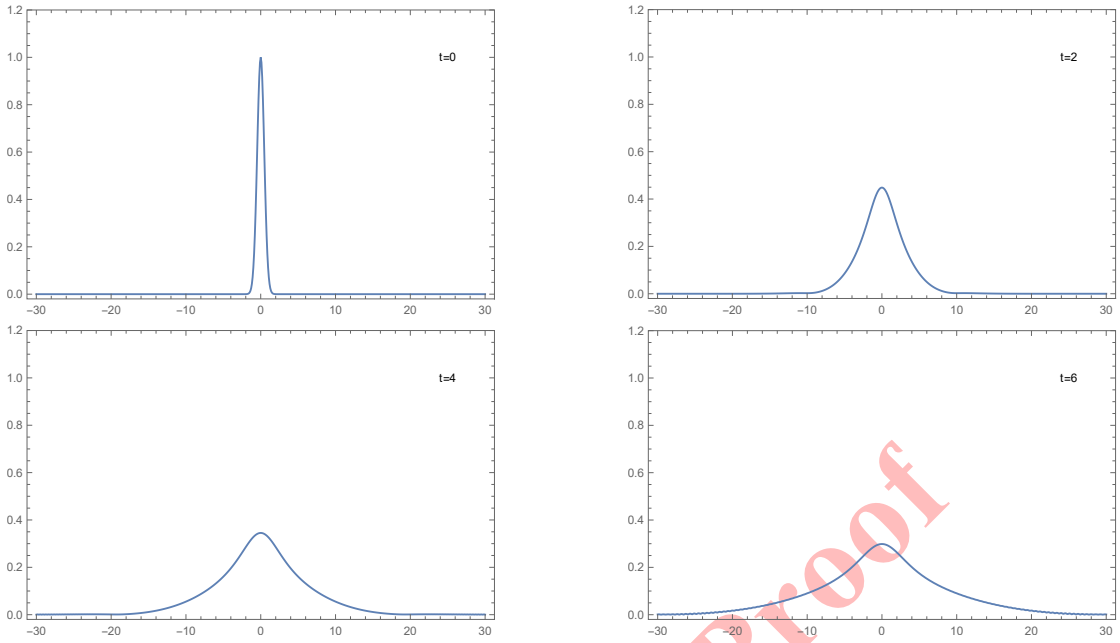


FIGURE 7. Standing soliton at $E = 1$.

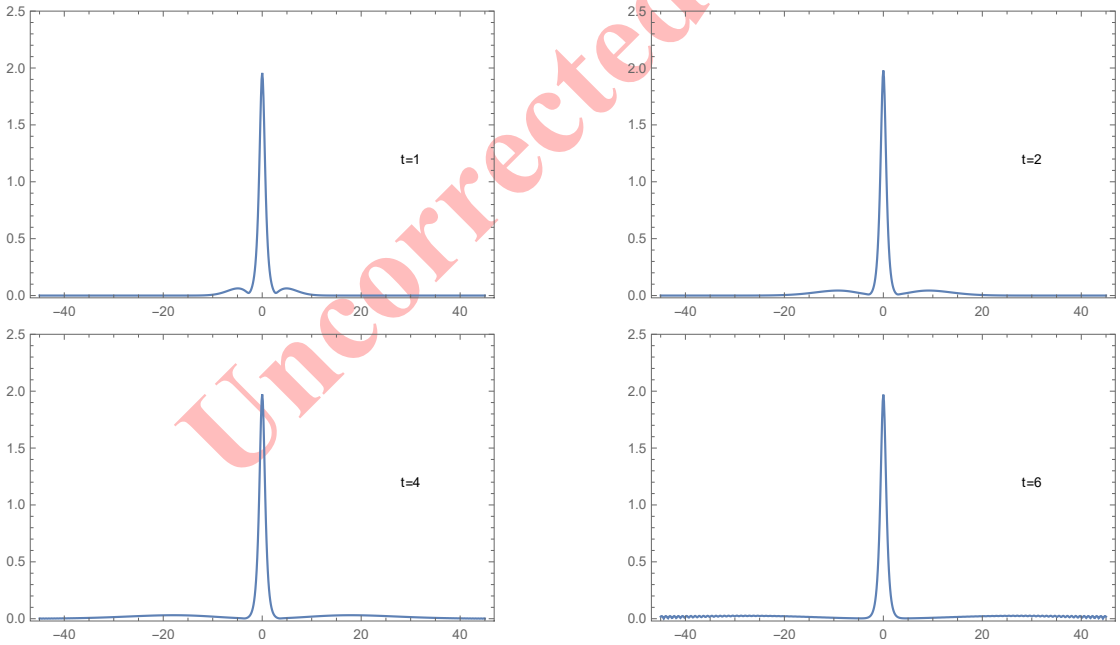


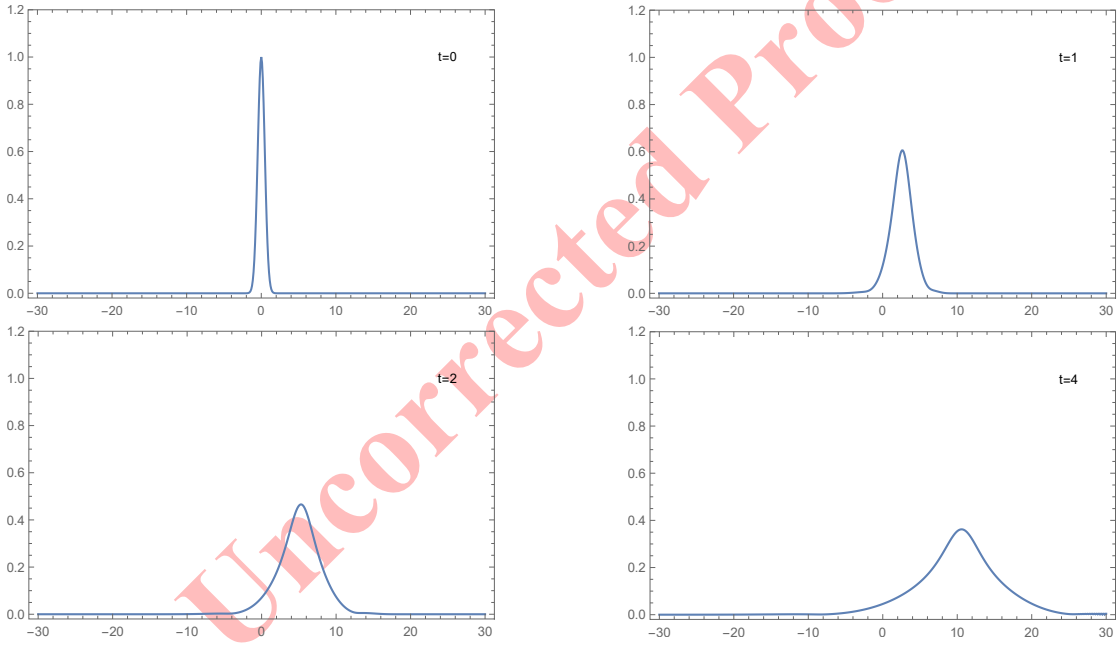
FIGURE 8. Standing soliton at $E = 1.78$.

speed throughout the simulation. Numerical values for $E = 1$ with $\Delta t = 0.01$, $N = 581$, as well as for $E = 1.78$ with $\Delta t = 0.005$, $N = 691$ are summarized in the Table 5 . The table demonstrates that the L-DQM yields two invariants, C_1 and C_2, which remain nearly constant and show good agreement.

Uncorrected Proof

TABLE 5. Invariants of mobile solitons at $E = 1$ and $E = 1.78$.

t	$E = 1$, $\Delta t = 0.01$, $N = 581$		$E = 1.78$, $\Delta t = 0.005$, $N = 691$	
	C_1	C_2	C_1	C_2
0.0	1.25239	5.37175	1.25239	5.37175
0.5	1.25258	5.35186	1.25258	5.35186
1.0	1.25268	5.34118	1.25268	5.34118
1.5	1.25272	5.33684	1.25272	5.33684
2.0	1.25274	5.33452	1.25274	5.33452
2.5	1.25276	5.33307	1.25276	5.33307
3.0	1.25276	5.33207	1.25276	5.33207
3.5	1.25277	5.33134	1.25277	5.33134
4.0	1.25278	5.33079	1.25278	5.33079
4.5	1.25278	5.33034	1.25278	5.33034
5.0	1.25279	5.32999	1.25279	5.32999
5.5	1.25290	5.32981	1.25290	5.32981



Uncorrected Proof

FIGURE 9. Mobile soliton at $E = 1$.

7. CONCLUSION

In this paper, we focused on the numerical approximation of the CNLS equation using L-DQM method. The spatial discretization is carried out through differentiation matrices constructed based on the L-DQM approach. We then solve the resulting system of ODEs in time t using the established RK4 method. This approach allows for the investigation of the motion of a single solitary wave. The results obtained are compared with the exact solution as well as with findings from previous studies. Interactions between two solitons have also been studied, revealing that the solitons maintain their identities after interaction. A standing soliton and a mobile soliton are also observed along with the figure, which clearly preserved the characteristic properties of solitons. The comparison of error norms with

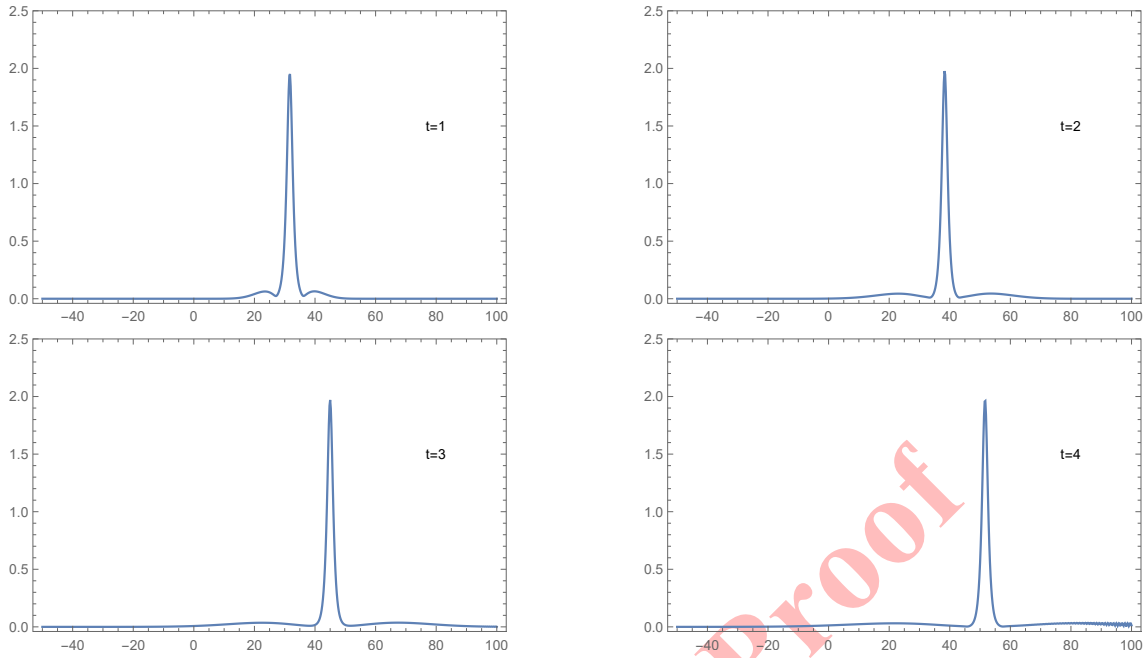


FIGURE 10. Mobile soliton at $E = 1.78$.

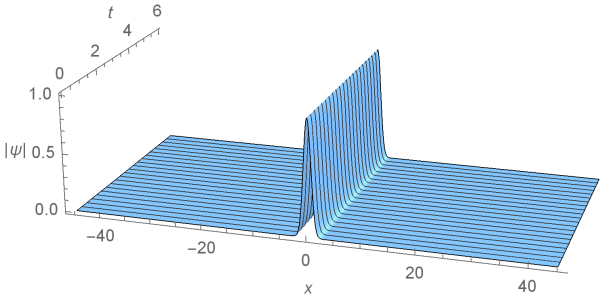


FIGURE 11. 3D of mobile soliton at $t = 1$.

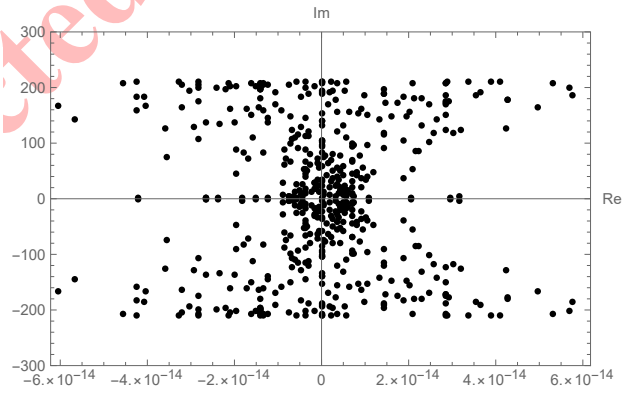


FIGURE 12. Eigen values for N=291.

Uncorrected Proof

earlier studies clearly demonstrates the superior accuracy and stability of the L-DQM method. Thus, the proposed technique proves to be a reliable and efficient numerical tool for solving the NLSE.

REFERENCES

[1] A. M. Aksoy, D. Irk, and I. Dag, *Taylor collocation method for the numerical solution of the nonlinear Schrödinger equation using quintic B-spline basis*, Physics of Wave Phenomena, *20*(1) (2012), 67-79.

[2] A. Başhan, *A mixed methods approach to Schrödinger equation: Finite difference method and quartic B-spline based differential quadrature method*, An International Journal of Optimization and Control: Theories & Applications (IJOCTA), *9*(2) (2019), 223-235.

[3] R. Bellman, B. Kashef, and J. Casti, *Differential quadrature: a technique for the rapid solution of nonlinear partial differential equations*, Journal of computational physics, *10*(1) (1972), 40-52.
[4] R. Bellman, B. Kashef, E. S. Lee, and R. Vasudevan, *Differential quadrature and splines*, Computers & Mathematics with Applications, *1*(3-4) (1975), 371-376.
[5] I. Dag, *Quadratic b-spline finite element method for solving nonlinear schrödinger equation*, Computer methods in applied mechanics and engineering, *174*(1-2) (1999), 247-258.
[6] M. Delfour, M. Fortin, and G. Payr, *Finite-difference solutions of a non-linear Schrödinger equation*, Journal of computational physics, *44*(2) (1981), 277-288.
[7] H. Demir and S. Sahin, *Numerical investigation of a steady flow of an incompressible fluid in a lid driven cavity*, Turkish Journal of Mathematics and Computer Science, *1* (2013), 14-23.
[8] L. R. T. Gardner, G. A. Gardner, S. I. Zaki, and Z. El Sahrawi, *B-spline finite element studies of the non-linear Schrödinger equation*, Computer methods in applied mechanics and engineering, *108*(3-4) (1993), 303-318.
[9] H. Hasimoto and H. Ono, *Nonlinear modulation of gravity waves*, Journal of the Physical Society of Japan, *33*(3) (1972), 805-811.
[10] G. M. Muslu and H. A. Erbay, *Higher-order split-step Fourier schemes for the generalized nonlinear Schrödinger equation*, Mathematics and Computers in Simulation, *67*(6) (2005), 581-595.
[11] J. R. Quan and C. T. Chang, *New insights in solving distributed system equations by the quadrature method—I. Analysis*, Computers & chemical engineering, *13*(7) (1989), 779-788.
[12] M. P. Robinson, *The solution of nonlinear Schrödinger equations using orthogonal spline collocation*, Computers & Mathematics with Applications, *33*(7) (1997), 39-57.
[13] B. Saka, *A quintic B-spline finite-element method for solving the nonlinear Schrödinger equation*, Physics of Wave Phenomena, *20*(2) (2012), 107-117.
[14] A. Shabat and V. Zakharov, *Exact theory of two-dimensional self-focusing and one-dimensional self-modulation of waves in nonlinear media*, Sov. Phys. JETP, *34*(1) (1972), 62.
[15] C. Shu, *Generalized differential-integral quadrature and application to the simulation of incompressible viscous flows including parallel computation*, University of Glasgow, United Kingdom, 1991.
[16] C. Shu, *Differential quadrature and its application in engineering*, Springer Science & Business Media, 2000 .
[17] C. Shu and B. E. Richards, *Application of generalized differential quadrature to solve two-dimensional incompressible Navier-Stokes equations*, International Journal for Numerical Methods in Fluids, *15*(7) (1992), 791-798.
[18] C. Shu and H. Xue, *Explicit computation of weighting coefficients in the harmonic differential quadrature*, Journal of Sound and Vibration, *204*(3) (1997), 549-555.
[19] G. F. Simmons, *Differential equations with applications and historical notes*, CRC Press, 2016.
[20] W. A. Strauss, *The nonlinear Schrödinger equation*, In North-Holland Mathematics Studies Vol. 30, North-Holland, 1978, 452-465.
[21] T. R. Taha and M. I. Ablowitz, *Analytical and numerical aspects of certain nonlinear evolution equations. II. Numerical, nonlinear Schrödinger equation*, Journal of computational physics, *55*(2) (1984), 203-230.
[22] E. H. Twizell, A. G. Bratsos, and J. C. Newby, *A finite-difference method for solving the cubic Schrödinger equation*, Mathematics and Computers in Simulation, *43*(1) (1997), 67-75.
[23] G. Yıgıt and M. Bayram, *Chebyshev differential quadrature for numerical solutions of higher order singular perturbation problems*, arXiv preprint arXiv:1705.09484, 2017.
[24] A. Yokus, H. M. Baskonus, T. A. Sulaiman, and H. Bulut, *Numerical simulation and solutions of the two-component second order KdV evolutionary system*, Numerical Methods for Partial Differential Equations, *34*(1) (2018), 211-227.
[25] A. Yokus, T. A. Sulaiman, H. M. Baskonus, and S. P. Atmaca, *On the exact and numerical solutions to a nonlinear model arising in mathematical biology*, ITM Web of Conferences, *22* (2018), 01061.

Uncorrected Proof